

A higher order numerical method for singularly perturbed elliptic problems with characteristic boundary layers

A. F. Hegarty ^{*} E. O’Riordan [†]

November 2, 2023

Abstract

A Petrov-Galerkin finite element method is constructed for a singularly perturbed elliptic problem in two space dimensions. The solution contains a regular boundary layer and two characteristic boundary layers. Exponential splines are used as test functions in one coordinate direction and are combined with bilinear trial functions defined on a Shishkin mesh. The resulting numerical method is shown to be a stable parameter-uniform numerical method that achieves a higher order of convergence compared to upwinding on the same mesh.

Keywords: Convection-diffusion, Shishkin mesh, Petrov-Galerkin, higher order.

AMS subject classifications: 65N12, 65N15, 65N06.

1 Introduction

Consider the following singularly perturbed elliptic problem: Find u such that, over the unit square $\Omega := (0, 1) \times (0, 1)$,

$$Lu := -\varepsilon\Delta u + a(x, y)u_x = f(x, y), \quad (x, y) \in \Omega; \quad 0 < \varepsilon \leq 1; \quad (1a)$$

$$u(x, y) = 0, \quad (x, y) \in \partial\Omega; \quad a \in C^{3,\lambda}(\bar{\Omega}); \quad a(x, y) > \alpha > 0, \quad (x, y) \in \bar{\Omega}. \quad (1b)$$

The complicated nature of the various boundary and corner layers that can appear in the solutions to (1) can be seen in the asymptotic expansions in

^{*}Department of Mathematics and Statistics, University of Limerick, Ireland.

[†]School of Mathematical Sciences, Dublin City University, Dublin 9, Ireland.

[11, pp.121-144] and [8], in the associated Green's function [6] and, even in the constant coefficient case of (1), in the bounding of the partial derivatives of various layer subcomponents [12] of the solution u . In this paper, we construct a stable parameter-uniform numerical method that achieves a higher order of parameter-uniform convergence compared to on the same Shishkin mesh as in [16] for problems of the form (1).

As the differential operator L in (1a) is inverse monotone ¹, we choose in this paper to only consider discretizations L^N of the differential operator L , which retain this fundamental property at all the mesh points $\bar{\Omega}^N$. Moreover, we are solely interested in parameter-uniform [5] inverse-monotone numerical methods. That is, inverse-monotone numerical methods for which an error bound on the global numerical approximations U of the form

$$\|u - U\| \leq CN^{-p}, \quad p > 0; \quad \|u\| := \max_{(x,y) \in \bar{\Omega}} |u(x,y)|$$

can be established. Here N is the number of elements used in any coordinate direction, $\|\cdot\|$ is the pointwise L_∞ norm and the error constant C (used throughout this paper) is independent of N and ε .

If f is sufficiently smooth ($f \in C^{1,\lambda}(\bar{\Omega})$) and satisfies sufficient compatibility at the four corners (see, e.g., [16]) then $u \in C^{3,\lambda}(\bar{\Omega})$ ². Assuming additional regularity ($f \in C^{5,\lambda}(\bar{\Omega})$) and additional compatibility conditions on the four corners [16], the solution u can be decomposed into a sum of a regular component $v \in C^{3,\lambda}(\bar{\Omega})$, and several layer components (all in the space $C^{3,\lambda}(\bar{\Omega})$)

$$u(x,y) = (v + w_E + w_S + w_{ES} + w_N + w_{EN})(x,y); \quad (2)$$

such that $Lv = f, Lw = 0$. The regular boundary layer w_E is significant along the east boundary $\partial\Omega_E := \{(1,y) | 0 \leq y \leq 1\}$. The characteristic boundary layers w_N and w_S occur, respectively along the north boundary $\partial\Omega_N := \{(x,1) | 0 \leq x \leq 1\}$ and south boundary $\partial\Omega_S := \{(x,0) | 0 \leq x \leq 1\}$. The corner layer functions w_{ES} and w_{EN} appear near the outflow corners $(1,0)$ and $(1,1)$. Rather stringent compatibility conditions (see [16]) can be imposed at the inflow corners $(0,0), (0,1)$ to prevent additional layers appearing along the north and south edges.

¹The differential operator L is inverse monotone in the sense that: for all $z \in C^0(\bar{\Omega}) \cup C^2(\Omega)$, if $z(x,y) \geq 0$, $(x,y) \in \partial\Omega$ and $Lz(x,y) \geq 0$, $(x,y) \in \Omega$ then $z(x,y) \geq 0$, $(x,y) \in \bar{\Omega}$.

²The space $C^\gamma(D)$ is the set of all functions that are Hölder continuous of degree γ with respect to the Euclidean norm $\|\cdot\|_e$. The space $C^{k,\gamma}(D)$ is the set of all functions in $C^k(D)$ whose derivatives of order k are Hölder continuous of degree γ .

As identified in [11, pp.123-126], the nature of the characteristic layers w_N and w_S are more complicated compared to the one dimensional character of the regular layer component w_E . The asymptotic character of the characteristic layer w_T is related to the solution z of the singularly perturbed parabolic problem [11]

$$\begin{aligned} -\varepsilon z_{yy} + az_x &= 0, & (x, y) \in (0, 1] \times (0, 1); \\ z(x, 0), z(x, 1); & x \in (0, 1), & z(0, y), y \in [0, 1] \text{ given.} \end{aligned}$$

In passing, it is worth noting that the standard energy norm ³ for problem (1) and the L^2 -norm are not appropriate norms [7] to identify the presence of these characteristic layers. A suitable balanced norm [7] could be used to avoid this defect, but by using the global pointwise norm $\|\cdot\|$ one avoids this issue altogether. Shishkin [18], [19] proved that, on a uniform mesh, no discretization will be parameter-uniform (in $\|\cdot\|$) for the above class of singularly perturbed parabolic problems, due to the presence (in general) of characteristic layers in the solution z . This negative result also holds for the class of elliptic problems [19] specified in (1). In addition, Shishkin [17] introduced piecewise-uniform meshes (now commonly called Shishkin meshes) which can be incorporated into a numerical method to produce parameter-uniform numerical methods both for problem (1) and for a wide class of singularly perturbed problems [5]. Below we will also use these Shishkin meshes to generate a numerical method that is parameter-uniform and of order higher than one for problem (1).

In the next section, we present bounds on the derivatives of the components in the decomposition (2) of the continuous solution of problem (1). In §3, we construct a fitted numerical method on a tensor product of two piecewise-uniform Shishkin meshes within a finite element framework. A suitable choice of quadrature rule generates an inverse-monotone numerical method. The numerical analysis of this method is conducted in §4 and the numerical performance of the scheme on several test examples is presented in §5. Some technical details of the truncation error analysis are presented in the appendix.

2 Continuous problem

For the solution decomposition (2) with some regularity and compatibility data constraints [16], we have the following bounds on the partial derivatives

³ $\|u\|_E^2 := \varepsilon\|u_x\|_{L^2}^2 + \varepsilon\|u_y\|_{L^2}^2 + \|u\|_{L^2}^2$, $\|u\|_{L^2}^2 := \int_{\Omega} z^2 d\Omega$,

of the components [16]:

$$\left\| \frac{\partial^{i+j} v}{\partial x^i \partial y^j} \right\| \leq C (1 + \varepsilon^{2-(i+j)}), \quad 0 \leq i + j \leq 3; \quad (3a)$$

$$|w_E(x, y)| \leq C e^{-\alpha \frac{1-x}{\varepsilon}}, \quad \left| \frac{\partial^i w_E(x, y)}{\partial x^i} \right| \leq C \varepsilon^{-i} e^{-\alpha \frac{1-x}{4\varepsilon}}, \quad 1 \leq i \leq 3; \quad (3b)$$

$$\left| \frac{\partial^j w_E(x, y)}{\partial y^j} \right| \leq C \varepsilon^{1-j} e^{-\alpha \frac{1-x}{4\varepsilon}}, \quad j = 2, 3; \quad (3c)$$

$$|w_S(x, y)| \leq C e^{-\frac{y}{\sqrt{\varepsilon}}}, \quad |w_N(x, y)| \leq C e^{-\frac{1-y}{\sqrt{\varepsilon}}}; \quad (3d)$$

$$\left| \frac{\partial^j w_S(x, y)}{\partial y^j} \right| \leq C \varepsilon^{-j/2} e^{-\frac{y}{\sqrt{\varepsilon}}}, \quad \left| \frac{\partial^j w_N(x, y)}{\partial y^j} \right| \leq C \varepsilon^{-j/2} e^{-\frac{1-y}{\sqrt{\varepsilon}}}, \quad j = 2, 3; \quad (3e)$$

$$\left| \frac{\partial^i w_S(x, y)}{\partial x^i} \right| \leq C \varepsilon^{2-i} e^{-\frac{y}{\sqrt{\varepsilon}}}, \quad \left| \frac{\partial^i w_N(x, y)}{\partial x^i} \right| \leq C \varepsilon^{2-i} e^{-\frac{1-y}{\sqrt{\varepsilon}}}, \quad i = 2, 3; \quad (3f)$$

and, for the corner layer functions,

$$|w_{ES}(x, y)| \leq C e^{-\alpha \frac{1-x}{2\varepsilon}} e^{-\frac{y}{\sqrt{\varepsilon}}}, \quad |w_{EN}(x, y)| \leq C e^{-\alpha \frac{1-x}{2\varepsilon}} e^{-\frac{1-y}{\sqrt{\varepsilon}}}; \quad (3g)$$

$$\left\| \frac{\partial^3 w_{ES}}{\partial y^3} \right\|, \left\| \frac{\partial^3 w_{EN}}{\partial y^3} \right\| \leq C \varepsilon^{-2}; \quad (3h)$$

$$\left\| \frac{\partial^i w_{ES}}{\partial x^i} \right\|, \left\| \frac{\partial^i w_{EN}}{\partial x^i} \right\| \leq C \varepsilon^{-i}, \quad i = 2, 3. \quad (3i)$$

These bounds on the derivatives of the components were used in [16] to establish first order uniform convergence (with a logarithmic defect) of a numerical method for problem (1). In the case of constant $a(x, y) = \alpha$, this result was improved in [1] where the severe compatibility restrictions (imposed in [16]) at the four corners were avoided. In [1], first order parameter-uniform convergence (with a logarithmic defect) at the nodes was retained, with the only requirement on the problem data being that the boundary data be continuous.

In this current paper we will examine a potentially higher order numerical scheme for the variable coefficient problem (1). Local compatibility conditions (at the four corners) and sufficient regularity on the data can be identified to ensure that the solution u and its subcomponents are in $C^{3,\lambda}(\bar{\Omega})$. In the case of constant $a(x, y) = \alpha$, local compatibility conditions can be specified at the four corners [12] so that $u \in C^{k+2,\lambda}(\bar{\Omega})$, $k > 0$ for $a, f \in C^{k,\lambda}(\bar{\Omega})$. However, in the general case of variable coefficients, local compatibility conditions cannot be identified to ensure $u \in C^{4,\lambda}(\bar{\Omega})$ (see the discussion in [9]) for problem (1). On the half-plane and for constant coefficients, Andreev [2] and Andreev and Belukhina [3] established bounds on a solution with no layers, without imposing any compatibility constraints. Using a partition of unity construction to link these two results

[2, 3] on the half-plane to the problem (1) posed on the unit square, Andreev and Belukhina [4] construct and appropriately bound a regular component $v \in C^{k+2,\lambda}(\bar{\Omega})$, $k > 0$ for $a, f \in C^{k,\lambda}(\bar{\Omega})$, without imposing any compatibility constraints on the data. However, for our purposes we require that all subcomponents in the decomposition (2) are in $C^{4,\lambda}(\bar{\Omega})$. To this end we shall simply assume that the solution u and all five of the layer functions are all in $C^{4,\lambda}(\bar{\Omega})$.

Assumption Assume that the problem data are such that

$$a, f \in C^{10,\lambda}(\bar{\Omega}); \quad (4a)$$

$$f(1, \ell) = 0, \quad \frac{\partial^{i+j} f}{\partial x^i \partial y^j}(0, \ell) = 0, \quad \ell = 0, 1; \quad 0 \leq i + j \leq 8; \quad (4b)$$

and for the components in the decomposition (2),

$$u, w_E, w_N, w_S, w_W, w_{EN}, w_{ES} \in C^{4,\lambda}(\bar{\Omega}). \quad (4c)$$

Using this assumption, we can extend the bounds in (3) to include the fourth derivatives of all the subcomponents. We also sharpen some of the bounds given in (3).

Lemma 1. *Assume (4). In addition to the bounds in (3) we have the following bounds:*

$$\left\| \frac{\partial^{i+j} v}{\partial x^i \partial y^j} \right\| \leq C(1 + \varepsilon^{3-(i+j)}), \quad 3 \leq i + j \leq 4; \quad (5a)$$

$$\left| \frac{\partial^i w_E(x, y)}{\partial x^i} \right| \leq C\varepsilon^{-i} e^{-\alpha \frac{1-x}{\varepsilon}}; \quad 1 \leq i \leq 4; \quad (5b)$$

$$\left| \frac{\partial^j w_E(x, y)}{\partial y^j} \right| \leq C\varepsilon^{2-j} e^{-\alpha \frac{1-x}{\varepsilon}}, \quad j = 3, 4; \quad (5c)$$

$$\left| \frac{\partial^i w_S(x, y)}{\partial x^i} \right| \leq C\varepsilon^{3-i} e^{-\frac{y}{\sqrt{\varepsilon}}}, \quad \left| \frac{\partial^i w_N(x, y)}{\partial x^i} \right| \leq C\varepsilon^{3-i} e^{-\frac{1-y}{\sqrt{\varepsilon}}}, \quad i = 3, 4; \quad (5d)$$

$$|w_{ES}(x, y)| \leq C e^{-\alpha \frac{1-x}{\varepsilon}} e^{-\frac{y}{\sqrt{\varepsilon}}}, \quad |w_{EN}(x, y)| \leq C e^{-\alpha \frac{1-x}{\varepsilon}} e^{-\frac{1-y}{\sqrt{\varepsilon}}}; \quad (5e)$$

$$\left| \frac{\partial^4 (w_{ES} + w_{EN})(x, y)}{\partial y^4} \right| \leq C\varepsilon^{-3} e^{-\alpha \frac{1-x}{\varepsilon}}, \quad \left| \frac{\partial^4 (w_{ES} + w_{EN})(x, y)}{\partial x^4} \right| \leq C\varepsilon^{-4} e^{-\alpha \frac{1-x}{\varepsilon}}. \quad (5f)$$

Proof. Consider the transformation $\tilde{u} := e^{-\frac{\alpha x}{2}} u$ and

$$\begin{aligned} \tilde{L}\tilde{u} &:= -\varepsilon \Delta \tilde{u} + \tilde{a}(x, y) \tilde{u}_x + \tilde{b}(x, y) \tilde{u} = \tilde{f}(x, y), \quad (x, y) \in \Omega, \\ \tilde{a}(x, y) &= (a(x, y) - \varepsilon \alpha) \geq \tilde{\alpha} > 0 \quad \tilde{b}(x, y) = (a(x, y) - \frac{\varepsilon \alpha}{2}) > 0 \quad \tilde{f} = e^{-\frac{\alpha x}{2}} f. \end{aligned}$$

From Andreev and Belukhina [4] a regular component $\tilde{v} \in C^{4,\lambda}(\bar{\Omega})$ can be constructed so that $\tilde{L}\tilde{v} = \tilde{f}$, $\tilde{v}(0, y) = 0$. Define $v := e^{\frac{\alpha x}{2}} \tilde{v} \in C^{4,\lambda}(\bar{\Omega})$ and

$Lv = f, v(0, y) = 0$. This regular component v can be decomposed (as in the constuction in [16]) so that

$$\begin{aligned} v^* &= v_0^* + \varepsilon v_1^* + \varepsilon^2 v_2^* + \varepsilon^3 v_3^*, \quad (x, y) \in \Omega^* = (0, 1 + d) \times (-d, 1 + d), \quad d > 0; \\ a^* \frac{\partial v_0^*}{\partial x} &= f^*; \quad a^* \frac{\partial v_i^*}{\partial x} = -\Delta v_{i-1}^*, \quad i = 1, 2; \quad x > 0; \\ v^*(0, y) &= u^*(0, y) \equiv 0, \quad v_i^*(0, y) = 0, \quad y \in [-d, 1 + d], \quad i = 1, 2 \quad \text{and} \\ L^* v_3^* &= -\Delta v_2^*, \quad v_3^*(x, y) = 0, \quad (x, y) \in \partial\Omega^*. \end{aligned}$$

Throughout this proof the z^* notation denotes an extension of the function z to a domain Ω^* that contains $\bar{\Omega}$ as a proper subdomain (see [16] for further details). Each subcomponent will require different extensions, but for notational simplicity, we denote all extensions simply by Ω^* . Given the assumptions (4b) on a, f we have $v_m \in C^{4,\lambda}(\bar{\Omega}), m = 0, 1, 2$ and then $v_3 \in C^{4,\lambda}(\bar{\Omega})$. Moreover, the restriction v of v^* to $\bar{\Omega}$ satisfies

$$Lv(x, y) = f(x, y), \quad (x, y) \in \Omega \quad \text{and} \quad v(0, y) = 0, \quad y \in [0, 1]. \quad (6)$$

On the other three sides of the boundary $\partial\Omega$, the regular component v takes its value from the above decomposition. The bounds (5a) on the regular component v follow as in [16].

The restriction w_E to $\bar{\Omega}$ of w_E^* (defined over the extended domain $[0, 1] \times [-d, 1 + d]$) satisfies

$$Lw_E(x, y) = 0, \quad (x, y) \in \Omega \quad \text{and} \quad (7)$$

$$w_E(0, y) = 0, \quad w_E(1, y) = (u - v)(1, y), \quad y \in [0, 1]. \quad (8)$$

From (3b), we have the following bound

$$|w_E(x, y)| \leq C e^{-\alpha \frac{1-x}{\varepsilon}}.$$

Consider the following decomposition of w_E^* :

$$w_E^*(x, y) = (u - v)^*(1, y) \phi^*(x, y) + \varepsilon^2 z_E^*(x, y),$$

where for all $y \in (-d, 1 + d), d > 0$, the function $\phi^*(x, y)$ is the solution of the boundary value problem

$$-\varepsilon \frac{\partial^2 \phi^*}{\partial x^2} + a^*(x, y) \frac{\partial \phi^*}{\partial x} = 0, \quad x \in (0, 1); \quad \phi^*(0, y) = 0, \quad \phi^*(1, y) = 1.$$

One can deduce that

$$\left| \frac{\partial^i \phi^*}{\partial x^i} \right| \leq C \varepsilon^{-i} e^{-\alpha \frac{1-x}{\varepsilon}} \quad \text{and} \quad \left| \frac{\partial^j \phi^*}{\partial y^j} \right| \leq C e^{-\alpha \frac{1-x}{\varepsilon}}.$$

Note that on the extended domain $z_E^* = 0, (x, y) \in \partial\Omega^*$ and

$$\varepsilon^2 L^* z_E = \varepsilon \frac{\partial^2}{\partial y^2} \left((u - v)^*(1, y) \phi^*(x, y) \right), \quad (x, y) \in \Omega^*,$$

which implies that $|L^* z_E| \leq C\varepsilon^{-1} e^{-\alpha \frac{1-x}{\varepsilon}}$. Use the arguments in [15, Chapter 12], coupled with the local bounds given in [13, pp. 132–134] and the arguments in [14], to deduce the bounds (5b) and (5c).

The restriction w_N to $\bar{\Omega}$ of w_N^* (defined over the extended domain $[0, 1] \times [-d, 1]$) satisfies

$$Lw_N(x, y) = 0, \quad (x, y) \in \Omega \quad \text{and} \quad w_N(0, y) = 0, \quad y \in [0, 1]; \quad (9a)$$

$$w_N(x, 0) = 0, \quad w_N(x, 1) = (u - v)(x, 1), \quad x \in [0, 1]. \quad (9b)$$

We consider the expansion of the top characteristic layer component

$$\begin{aligned} w_N^* &= w_0^* + \varepsilon w_1^* + \varepsilon^2 w_2^* + \varepsilon^3 w_3^*, \quad \text{where} \\ L_p^* w_0^* &:= -\varepsilon (w_0^*)_{yy} + a^*(x, y) (w_0^*)_x = 0, \quad (x, y) \in (0, 1 + d) \times (0, 1); \\ w_0^*(0, y) &= w_0^*(x, 0) = 0, \quad w_0^*(x, 1) = -(v_0^* + \varepsilon v_1^* + \varepsilon^2 v_2^*)(x, 1); \\ L_p^* w_i^* &= (w_{i-1}^*)_{xx}, \quad (x, y) \in (0, 1 + d) \times (0, 1), \\ w_i^*(0, y) &= w_i^*(x, 0) = w_i^*(0, 1) = 0, \quad i = 1, 2; \\ L^* w_3^* &= (w_2^*)_{xx}, \quad (x, y) \in (0, 1 + d) \times (0, 1); \\ w_3^*(0, y) &= w_3^*(x, 0) = w_3^*(1 + d, 0) = 0, \quad w_3^*(x, 1) = -v_3^*(x, 1). \end{aligned}$$

Using the assumptions (4b) on the data coupled with extending the argument in [16, Lemma 3] one can deduce that $w_m^* \in C^{12-2m+2\lambda}(\bar{\Omega})$, $m = 0, 1, 2$.⁴ By (4c), $w_N \in C^{4,\lambda}(\bar{\Omega})$ and $w_m \in C^{4,\lambda}(\bar{\Omega})$, $\lambda < 0.5$, $m = 0, 1, 2$ which implies $w_3 \in C^{4,\lambda}(\bar{\Omega})$, $\lambda < 0.5$. The bounds (5d) on w_N , and analogously w_S , follow as in [16].

The corner layer function w_{EN} satisfies

$$Lw_{EN}(x, y) = 0, \quad (x, y) \in \Omega \quad \text{and} \quad (10a)$$

$$w_{EN}(0, y) = 0, \quad w_{EN}(1, y) = -w_N(1, y), \quad y \in [0, 1]; \quad (10b)$$

$$w_{EN}(x, 0) = 0, \quad w_{EN}(x, 1) = -w_E(x, 1), \quad x \in [0, 1]. \quad (10c)$$

⁴The space $C^{0+\gamma}(D)$ is the set of all functions that are Hölder continuous of degree γ with respect to the metric $d(\vec{u}, \vec{v}) := \sqrt{(u_1 - v_1)^2 + |u_2 - v_2|}$, $\forall \vec{u}, \vec{v} \in R^2$. Moreover,

$$C^{n+\gamma}(D) := \left\{ z : \frac{\partial^{i+j} z}{\partial x^i \partial y^j} \in C^{0+\gamma}(D), 0 \leq i + 2j \leq n \right\}.$$

For ε sufficiently small and using the strict inequality $a > \alpha$ we have that

$$Le^{-\alpha\frac{1-x}{\varepsilon}}e^{-\frac{1-y}{\sqrt{\varepsilon}}} = \frac{1}{\varepsilon}(\alpha(a(x,y) - \alpha) - \varepsilon)e^{-\alpha\frac{1-x}{\varepsilon}}e^{-\frac{1-y}{\sqrt{\varepsilon}}} \geq 0.$$

This yields the bounds in (5e). The bounds in (5f) are established by using the expansion

$$\begin{aligned} w_{EN}(x,y) &= w_N(1,y)B_E(x) - \left(w_E(x,1) + w_E(1,1)B_E(x)\right)B_N(y) + \varepsilon z_{EN}(x,y), \\ -\varepsilon B_E''(x) + a(1,1)B_E'(x) &= 0, \quad x \in (0,1) \quad B_E(0) = 0, \quad B_E(1) = -1, \\ -\varepsilon B_N''(y) + B_N(y) &= 0, \quad y \in (0,1) \quad B_N(0) = 0, \quad B_N(1) = 1. \end{aligned}$$

and extending the argument in [16] to include the fourth derivatives. The bounds on w_{ES} are established in an analogous fashion. \square

Remark 1. *In certain circumstances the bounds in (5c) can be sharpened to*

$$\left| \frac{\partial^j w_E(x,y)}{\partial y^j} \right| \leq C\varepsilon^{3-j}e^{-\alpha\frac{1-x}{\varepsilon}}, \quad j = 3, 4. \quad (11)$$

For example, if $a_y(x,y) \equiv 0$ and $f_{yy}(x,y) \equiv 0$ for all $(x,y) \in \Omega$, then $(v_0)_{yy}(x,y) = 0$ and $\phi^*(x)$ is independent of the vertical variable y . In this case, the remainder term Z_E in the expansion of w_E will satisfy $|L^*z_E| \leq Ce^{-\alpha\frac{1-x}{\varepsilon}}$. Using this bound in the above proof of the bound (5c) will result in the bound (11) being deduced.

3 Finite element framework

A weak form of problem (1) is: find $u \in H_0^1(\Omega)$ such that

$$B(u,v) := (\varepsilon \nabla u, \nabla v) + (au_x, v) = (f, v), \quad \forall v \in H_0^1(\Omega); \quad (12)$$

where (u,v) is the standard inner product in $L_2(\Omega)$ and $H_0^1(\Omega) := \{v | v, v_x, v_y \in L_2(\Omega), v(x,y) = 0 \text{ for } (x,y) \in \partial\Omega\}$.

The domain is discretized $\bar{\Omega} = \cup_{i,j=1}^{N,M} \bar{\Omega}_{i,j}$ by the rectangular elements

$$\bar{\Omega}_{i,j} := [x_{i-1}, x_i] \times [y_{j-1}, y_j], \quad 1 \leq i \leq N, \quad 1 \leq j \leq M;$$

where the internal nodal points are given by the following sets

$$\omega_x := \{x_i | x_i = x_{i-1} + h_i\}_{i=1}^{N-1} \quad \omega_y := \{y_j | y_j = y_{j-1} + k_j\}_{j=1}^{M-1}.$$

We define the average mesh steps with

$$\bar{h}_i := \frac{h_{i+1} + h_i}{2}, \quad \bar{k}_j := \frac{k_{j+1} + k_j}{2}.$$

This mesh is a tensor product of two piecewise-uniform one dimensional Shishkin meshes [15]. That is $\bar{\Omega}^N := \bar{\omega}_x \times \bar{\omega}_y$. The horizontal mesh $\bar{\omega}_x$ places $N/2$ elements into both $[0, 1 - \tau_x]$ and $[1 - \tau_x, 1]$ and the vertical mesh distributes M mesh points in the ratio 1 : 2 : 1 across the three subintervals $[0, \tau_y]$, $[\tau_y, 1 - \tau_y]$ and $[1 - \tau_y, 1]$. Based on the exponential pointwise bounds on the layer components, the transition parameters τ_x, τ_y are taken to be

$$\tau_x = \min\{0.5, 2\frac{\varepsilon}{\alpha} \ln N\} \quad \text{and} \quad \tau_y = \min\{0.25, 2\sqrt{\varepsilon} \ln M\}. \quad (13)$$

This Shishkin mesh has an additional factor of 2 in the transition points, compared to the mesh used in [1] and [16].

In the case of non-constant a, f , we will approximate the integrals in the weak form, by replacing a, f by piecewise constant functions in each subregion $Q_{i,j} := (x_{i-1}, x_{i+1}) \times (y_{j-1}, y_j)$ and then evaluating the integrals exactly. That is, we define the piecewise constant functions: For $(x, y) \in Q_{i,j}$, we define

$$\bar{a}(x, y) = \begin{cases} \bar{a}_i(y_j), & x_{i-1} < x \leq x_i \\ \bar{a}_{i+1}(y_j), & x_i < x \leq x_{i+1} \end{cases} \quad \bar{a}_i(y_j) := \frac{a(x_{i-1}, y_j) + a(x_i, y_j)}{2}.$$

The approximation \bar{f} is defined in an analogous fashion. In addition, we will lump all zero order terms, which yields increased stability and gives a simpler structure to the definition of the system matrix. That is, we introduce the additional quadrature rule

$$\left(a \frac{\partial \phi_{n,m}}{\partial x}, \psi_{i,j}\right) \approx \left(\bar{a} \frac{\partial \phi_n}{\partial x}(x), \psi_i(x)\right) (1, \psi^j(y)) \delta_{m,j},$$

where $\delta_{i,j}$ is the Kronecker delta. Then we have the following quadrature rules:

$$(\bar{a} U_x, V) := \sum_{j=1}^M (\bar{a}(y_j) U_x(x, y_j), V(x, y_j)) \bar{k}_j, \quad (\bar{f}, V) := \sum_{j=1}^M (\bar{f}(y_j), V(x, y_j)) \bar{k}_j.$$

The trial and test space will be denoted by $S^N, T^N \subset H_0^1(\Omega)$, respectively. The trial functions $\{\phi_{i,j}(x, y) := \phi_i(x) \phi^j(y)\}_{i,j=1}^{N-1, M-1} \in S^N$, are simply a tensor product of one dimensional hat functions. Motivated by ([10]), the

test functions $\{\psi_{i,j}(x, y) := \psi_i(x)\psi^j(y)\}_{i,j=1}^{N-1, M-1} \in T^N$ are a tensor product of exponential basis functions in the horizontal and hat functions in the vertical direction. That is, the basis functions $\psi_i(x)$ are the solutions of

$$\varepsilon \frac{\partial^2 \psi_i}{\partial x^2} + \bar{a}_i(y_j) \frac{\partial \psi_i}{\partial x} = 0, \quad \psi_i(x_j) = \delta_{i,j}.$$

An approximate solution $U \in S^N$ to the solution of problem (12) is: find $U \in S^N$ such that

$$\bar{B}(U, \psi_{i,j}) = (\bar{f}, \psi_{i,j}), \quad \forall \psi_{i,j} \in T^N; \quad (14a)$$

$$\text{where } \bar{B}(U, V) := \varepsilon(U_x, V_x) + \varepsilon(U_y, V_y) + (\bar{a}U_x, V). \quad (14b)$$

We denote the nodal values $U(x_i, y_j)$ simply by $U_{i,j}$. Hence

$$U(x, y) = \sum_{i,j=1}^N U_{i,j} \phi_i(x) \phi^j(y).$$

The associated finite difference scheme to this finite element method is:

$$\begin{aligned} L^N U_{i,j} &:= \frac{1}{\bar{h}_i} (-\varepsilon h_{i+1} D_x^+ (\sigma(-\rho_{i,j}) D_x^-) - \varepsilon Q_{i,j}^C \delta_y^2 + \bar{a} h_i D_x^-) U_{i,j} \\ &= \frac{1}{\bar{h}_i} (Q_{i,j}^- \bar{f}_{i,j} + Q_{i,j}^+ \bar{f}_{i+1,j}), \quad \text{where } Q_{i,j}^C := Q_{i,j}^- + Q_{i,j}^+, \end{aligned} \quad (15a)$$

$$Q_{i,j}^- := h_i \frac{\sigma(\rho_{i,j}) - 1}{\rho_{i,j}}, \quad Q_{i,j}^+ := h_{i+1} \frac{1 - \sigma(-\rho_{i+1,j})}{\rho_{i+1,j}}, \quad (15b)$$

$$\rho_{i,j} := \frac{\bar{a}_i(y_j) h_i}{\varepsilon} \quad \text{and} \quad \sigma(x) := \frac{x}{1 - e^{-x}}. \quad (15c)$$

Lemma 2. (*Discrete Minimum Principle*) *If Z is a mesh function defined at all mesh points $(x_i, y_j) \in \bar{\Omega}^N$, with $Z_{i,j} \geq 0$, $(x_i, y_j) \in \partial\Omega^N$ and $L^N Z_{i,j} \geq 0$, $(x_i, y_j) \in \Omega^N$ then $Z_{i,j} \geq 0$, $(x_i, y_j) \in \bar{\Omega}^N$.*

Proof. Use the standard proof-by-contradiction argument coupled with the fact that $\sigma(x) > 0, \forall x$. \square

Corollary 1. *If $Z(x_i)$ is such that $D_x^- Z(x_j) \geq 0, \forall x_j \in \omega_x$ then*

$$L^N Z(x_i) \geq \frac{\alpha}{1 - e^{-\bar{\rho}_{i+1}}} (D_x^- Z(x_i) - e^{-\bar{\rho}_{i+1}} D_x^+ Z(x_i)), \quad \text{where } \bar{\rho}_i := \frac{\alpha h_i}{\varepsilon}$$

Proof. On the mesh $\bar{\Omega}^N$, $h_i \geq \bar{h}_i \geq h_{i+1}$ and $\sigma'(x) > 0$, Hence

$$\begin{aligned} L^N Z(x_i) &\geq \frac{\varepsilon}{h_i} \sigma(\bar{\rho}_i) D_x^- Z(x_i) - \frac{\varepsilon}{h_{i+1}} \sigma(-\bar{\rho}_{i+1}) D_x^+ Z(x_i) \\ &\geq \frac{\alpha}{1 - e^{-\bar{\rho}_{i+1}}} (D_x^- Z(x_i) - e^{-\bar{\rho}_{i+1}} D_x^+ Z(x_i)), \end{aligned}$$

\square

4 Error analysis

The discrete solution U of (14) can be decomposed in an analogous fashion to the continuous solution. We write

$$U = V + W_E + W_N + W_S + W_{EN} + W_{ES}.$$

The nodal values of the discrete regular component V satisfy

$$L^N V = f(x_i, y_j), (x_i, y_j) \in \Omega^N, V = v(x_i, y_j), (x_i, y_j) \in \partial\Omega^N \quad (16a)$$

and the nodal values of each of the layer functions W satisfy

$$L^N W(x_i, y_j) = 0, (x_i, y_j) \in \Omega^N, W = w(x_i, y_j), (x_i, y_j) \in \partial\Omega^N. \quad (16b)$$

Lemma 3. *Assume (4). The approximation V satisfies the nodal error bound*

$$|(V - v)(x_i, y_j)| \leq C(N^{-2} + M^{-2}(1 + \sqrt{\varepsilon} \ln M)), \quad (x_i, y_j) \in \Omega^N;$$

where v solves the problem specified in (6).

Proof. Using the bounds (5) on the regular component and the truncation error bounds (31), (32) from the Appendix yields

$$|L^N(V - v)(x_i, y_j)| \leq C \begin{cases} N^{-2} + M^{-2} + \varepsilon|k_j - k_{j+1}| & \text{if } h_i = h_{i+1} \\ N^{-1} + M^{-2} + \varepsilon|k_j - k_{j+1}| & \text{if } h_i \neq h_{i+1} \end{cases}.$$

Let us examine the following three barrier functions

$$B_1(x_i, y_j) = x_i, \quad B_2(x_i, y_j) = \begin{cases} \frac{y_j}{\tau_y} & y_j < \tau_y \\ 1, & \tau_y \leq y_j \leq 1 - \tau_y \\ \frac{1-y_j}{1-\tau_y} & y_j > 1 - \tau_y \end{cases} \quad (17a)$$

$$B_3(x_i, y_j) = \begin{cases} e^{-\frac{\alpha(1-\tau_x-x_i)i}{2\varepsilon}}, & x_i \leq 1 - \tau_x \\ 1 & x_i > 1 - \tau_x \end{cases}. \quad (17b)$$

Observe that,

$$L^N B_1 = \frac{\varepsilon}{\bar{h}_i} (\sigma(-\rho_{i,j}) + \rho_{i,j} - \sigma(-\rho_{i+1,j})) = \frac{\varepsilon}{\bar{h}_i} (\sigma(\rho_{i,j}) - \sigma(-\rho_{i+1,j})) \geq 0, \quad \forall i;$$

$$L^N B_1 = \frac{\varepsilon}{\bar{h}_i} (\sigma(-\rho_{i,j}) - \sigma(-\rho_{i+1,j}) + \rho_{i,j}) \geq \alpha + O(h_i) \geq \frac{\alpha}{2}, \quad x_i \neq 1 - \tau_x;$$

$$-\varepsilon \delta_y^2 B_2 = 0, y_j \neq \tau_y, 1 - \tau_y \quad -\varepsilon \delta_y^2 B_2 = \frac{\sqrt{\varepsilon} M}{8 \ln M}, y_j = \tau_y, 1 - \tau_y;$$

$$L^N B_3 \geq \frac{\varepsilon}{H} (\sigma(\rho_{i,j}) - \sigma(-\rho_{i+1,j}) e^{-\frac{\alpha H}{2\varepsilon}}) D_x^- B_3 \geq 0, \quad x_i < 1 - \tau_x, \quad \text{as } \frac{x e^{-x/2}}{1 - e^{-x}} \leq 1;$$

$$\text{and at } x_i = 1 - \tau_x \quad L^N B_3 \geq \frac{2\alpha}{\bar{h}_i} \frac{\sigma(\rho_i)}{\sigma(\frac{\alpha H}{2\varepsilon})} \geq CN.$$

To complete the proof construct the barrier function

$$C(N^{-2} + M^{-2})B_1(x_i) + C\sqrt{\varepsilon}M^{-2} \ln MB_2(x_i) + CN^{-2}B_3(x_i)$$

where the functions $B_m(x_i), m = 1, 2, 3$ are defined in (17). \square

Lemma 4. *Assume (4). At each mesh point $(x_i, y_j) \in \Omega^N$, the approximation W_E satisfies the nodal error bound*

$$|(W_E - w_E)(x_i, y_j)| \leq C(N^{-1} \ln N)^2 + CM^{-1}(M^{-1} \ln M)^{\frac{2}{3}}, \quad (18a)$$

where w_E solves the problem specified in (7). If the bound (11) is valid then

$$|(W_E - w_E)(x_i, y_j)| \leq C(N^{-1} \ln N)^2 + C(M^{-1} \ln M)^2. \quad (18b)$$

Proof. From Corollary 1, at all internal mesh points, we have that

$$L^N e^{-\frac{\alpha(1-x_i)}{\varepsilon}} \geq \frac{\alpha(1 - e^{-\bar{\rho}_i})}{1 - e^{-\bar{\rho}_{i+1}}} e^{-\frac{\alpha(1-x_i)}{\varepsilon}} \geq 0.$$

Hence, using the bound (5b) to bound $w_E(x, 0), w_E(x, 1)$ and the discrete minimum principle, we have the following bound

$$|W_E(x_i, y_j)| \leq C e^{-\frac{\alpha(1-x_i)}{\varepsilon}}, \quad \forall (x_i, y_j) \in \Omega^N.$$

Observe that in the case where the horizontal mesh is a uniform mesh (i.e., $\tau_x = 0.5$), then $e^{-\frac{\alpha\tau_x}{\varepsilon}} \leq N^{-2}$.

Also, by the choice of the transition parameter τ_x in (13) and the point-wise bound (5b) on the layer component

$$|w_E(x_i, y_j)| \leq CN^{-2}, \quad \text{if } x_i \leq 1 - \tau_x.$$

Hence, for the mesh points outside the right boundary layer region,

$$|(W_E - w_E)(x_i, y_j)| \leq CN^{-2}, \quad \text{for } x_i \leq 1 - \tau_x.$$

For mesh points within the side region $(1 - \tau_x, 1) \times (0, 1)$, using the bounds (5b) and (5c) we have that the truncation error, along each level $y = y_j$, is

$$|L^N(W_E - w_E)(x_i, y_j)| \leq C \frac{(N^{-1} \ln N)^2}{\varepsilon} e^{-\alpha \frac{1-x_i}{\varepsilon}} + C e^{-\alpha \frac{1-x_i}{\varepsilon}} \begin{cases} |k_j - k_{j+1}|, & k_j \neq k_{j+1} \\ \varepsilon^{-1} k_j^2, & k_j = k_{j+1} \end{cases}$$

in both the case of $\tau_x < 0.5$ and the case of $\tau_x = 0.5$. At all internal mesh points

$$\begin{aligned} L^N e^{-\frac{\alpha(1-x_i)}{2\varepsilon}} &\geq \frac{\alpha}{2\bar{h}_i} \left(\frac{\sigma(\rho_i)}{\sigma(\bar{\rho}_i/2)} - \frac{\sigma(-\rho_{i+1})}{\sigma(-\bar{\rho}_{i+1}/2)} \right) e^{-\frac{\alpha(1-x_i)}{2\varepsilon}} \\ &\geq \frac{C}{\bar{h}_i} (1 - e^{-\bar{\rho}_i/2}) e^{-\frac{\alpha(1-x_i)}{2\varepsilon}} > 0, \quad \text{as } \sigma'(x) > 0. \end{aligned}$$

Note in the special case where $\tau_x = 0.5$ and the mesh is uniform then we use that in this case $\sigma(\rho) \leq C$. In the other case, complete the proof of the bound (18a), with the barrier function ($B_2(x_i)$ is defined in (17)):

$$C(N^{-1} \ln N)^2 + (M^{-1} \ln M)^2 e^{-\frac{\alpha(1-x_i)}{2\varepsilon}} + C \min \left\{ \frac{M^{-2} \ln M}{\sqrt{\varepsilon}} B_2(x_i), \varepsilon M^{-1} e^{-\frac{\alpha(1-x_i)}{2\varepsilon}} \right\},$$

as the minimum is reached when $\varepsilon = (M^{-1} \ln M)^{2/3}$. If the bound (11) is valid then the truncation error is

$$|L^N(W_E - w_E)(x_i, y_j)| \leq C e^{-\alpha \frac{1-x_i}{\varepsilon}} \left(\frac{(N^{-1} \ln N)^2}{\varepsilon} + \begin{cases} \varepsilon |k_j - k_{j+1}|, & k_j \neq k_{j+1} \\ k_j^2, & k_j = k_{j+1} \end{cases} \right)$$

and the bound (18b) will follow. \square

Lemma 5. *Assume (4), then for all $(x_i, y_j) \in \Omega^N$*

$$|(W_N - w_N)(x_i, y_j)| \leq C(N^{-1} \ln N)^2 + C(M^{-1} \ln M)^2, \quad (19a)$$

$$|(W_S - w_S)(x_i, y_j)| \leq C(N^{-1} \ln N)^2 + C(M^{-1} \ln M)^2; \quad (19b)$$

where the characteristic layer function w_N solves the problem specified in (9).

Proof. From Corollary 1, we have that at all internal mesh points

$$L^N e^{\frac{2x_i}{\alpha}} \geq 2 \left(\frac{1}{\sigma(2h_i/\alpha)} - \frac{e^{-\frac{\alpha}{\varepsilon}(1-\frac{2\varepsilon}{\alpha^2})h_{i+1}}}{\sigma(2h_{i+1}/\alpha)} \right) e^{\frac{2x_i}{\alpha}}.$$

Then for ε sufficiently small ($4\varepsilon < \alpha^2$) and N sufficiently large (independently of ε) we have that

$$L^N e^{\frac{2x_i}{\alpha}} \geq e^{\frac{2x_i}{\alpha}}.$$

Consider the one dimensional barrier function $\Phi(y_j)$ defined by

$$-\varepsilon \delta_y^2 \Phi(y_j) + \Phi(y_j) = 0, \quad y_j \in \omega_j; \quad \Phi(0) = 0, \quad \Phi(1) = 1, \quad (20)$$

which approximates $-\varepsilon \phi'' + \phi = 0, y \in (0, 1), \phi(0) = 0, \phi(1) = 1$. Then [14]

$$|\Phi(y_j) - \phi(y_j)| \leq CM^{-2}(\ln M)^2, \quad \forall y_j \in (0, 1).$$

Now we form the two dimensional barrier function $e^{\frac{2x_i}{\alpha}} \Phi(y_j)$ which satisfies

$$L^N e^{\frac{2x_i}{\alpha}} \Phi(y_j) \geq 0, \quad |W_N(1, y_j)| = |w_N(1, y_j)| \leq Ce^{-\frac{(1-y_j)}{\sqrt{\varepsilon}}} \leq C\Phi(y_j) + CM^{-2}(\ln M)^2.$$

Hence, $|W_N(x_i, y_j)| \leq Ce^{\frac{2x_i}{\alpha}} \Phi(y_j)$. Then,

$$|(W_N - w_N)(x_i, y_j)| \leq |W_N(x_i, y_j)| + |w_N(x_i, y_j)| \leq CM^{-2}(\ln M)^2, \quad y_j \leq 1 - \tau_y.$$

For $y_j > 1 - \tau_y$ the truncation error is

$$|L^N(W_N - w_N)(x_i, y_j)| \leq CM^{-2}(\ln M)^2 + C \begin{cases} N^{-1}, h_i \neq h_{i+1} \\ \frac{h_i^2}{\varepsilon} e^{-\alpha \frac{1-x}{\varepsilon}}, h_i = h_{i+1} \end{cases}.$$

Note in the special case where $\tau_y = 0.25$, and the vertical mesh is uniform, we use $\varepsilon^{-1} \leq C(\ln M)^2$. In the other case, complete the proof with the barrier function

$$C(N^{-1} \ln N)^2 e^{-\frac{\alpha(1-x_i)}{2\varepsilon}} + C(M^{-1} \ln M)^2 x_i + CN^{-1} B_3(x_i).$$

□

Lemma 6. Assume (4), then for all $(x_i, y_j) \in \Omega^N$

$$|(W_{EN} - w_{EN})(x_i, y_j)| \leq C(N^{-1} \ln N)^2 + C(M^{-1} \ln M)^2; \quad (21a)$$

$$|(W_{ES} - w_{ES})(x_i, y_j)| \leq C(N^{-1} \ln N)^2 + C(M^{-1} \ln M)^2, \quad (21b)$$

where the corner layer function w_{EN} solves the problem specified in (10).

Proof. Using the discrete minimum principle we have that

$$\begin{aligned} |W_{EN}(x_i, y_j)| &\leq C e^{-\frac{\alpha(1-x_i)}{\varepsilon}}, \quad x_i \leq 1 - \tau_x; \\ |W_{EN}(x_i, y_j)| &\leq C e^{\frac{2x_i}{\alpha}} \Phi(y_j) + CM^{-2}(\ln M)^2, \quad y_j \leq 1 - \tau_y, \end{aligned}$$

where Φ is defined in (20). In the fine corner mesh where $x_i > 1 - \tau_x$ and $y_j > 1 - \tau_y$ the truncation error is

$$|L^N(W_{EN} - w_{EN})(x_i, y_j)| \leq C\varepsilon^{-1} \left(N^{-2}(\ln N)^2 + M^{-2}(\ln M)^2 \right) e^{-\alpha \frac{1-x_i}{\varepsilon}}.$$

Complete the proof with the barrier function

$$C((N^{-1} \ln N)^2 + (M^{-1} \ln M)^2) e^{-\alpha \frac{1-x_i}{2\varepsilon}} + C(N^{-1} \ln N)^2 + C(M^{-1} \ln M)^2.$$

□

On the Shishkin mesh Ω^N , these nodal error bounds easily extended to a global error bound. Using the triangle inequality and the interpolation bound [20, Theorem4.2]

$$\|u - u_I\| \leq C(N^{-1} \ln N)^2 + C(M^{-1} \ln M)^2,$$

where u_I is the bilinear interpolants of the exact solution u on the Shishkin mesh. Then, collecting together all the error bounds on the components established in Lemma 3-6, we easily deduce the following global error bound.

Theorem 1. (*Global convergence*) Assume (4). We have the error bound

$$\|U - u\| \leq C(N^{-1} \ln N)^2 + CM^{-1}(M^{-1} \ln M)^{\frac{2}{3}}$$

and if the bound (11) is valid then

$$\|U - u\| \leq C(N^{-1} \ln N)^2 + C(M^{-1} \ln M)^2. \quad (22)$$

Here U is the solution of (14) and u is the solution of (1).

5 Numerical examples

In this final section, we estimate the global accuracy of the fitted scheme (14), when it is applied to three test problems. In all three test problems, we relax the theoretical data constraints imposed in Assumption (4).

For convenience, we have simply taken $M = N$ in all of these numerical experiments and the global orders of local convergence are estimated using the double-mesh principle [5, §8.6]. For each particular value of $\varepsilon \in R_\varepsilon := \{2^{-i}, i = 0, 1, 2, \dots, 20\}$ and $N \in R_N := \{2^{-j}, j = 3, 4, 5 \dots 10\}$, let $U^N(x_i, y_j)$ denote the nodal values of the computed solution and \bar{U}^N is the bilinear interpolant of these nodal values, where N denotes the number of mesh elements used in each co-ordinate direction. Define the maximum local two-mesh global differences D_ε^N and the parameter-uniform two-mesh global differences D^N by

$$D_\varepsilon^N := \|\bar{U}^N - \bar{U}^{2N}\| \quad \text{and} \quad D^N := \max_{\varepsilon \in R_\varepsilon} D_\varepsilon^N.$$

Then, for any particular value of ε and N , the local orders of global convergence are denoted by \bar{p}_ε^N and, for any particular value of N and *all values* of ε , the parameter-uniform global orders of convergence \bar{p}^N are defined, respectively, by

$$\bar{p}_\varepsilon^N := \log_2 \left(\frac{D_\varepsilon^N}{D_\varepsilon^{2N}} \right) \quad \text{and} \quad \bar{p}^N := \log_2 \left(\frac{D^N}{D^{2N}} \right).$$

In the classical case of $\varepsilon = 1$ we observe global orders approaching two for the fitted scheme (14) applied to all the test problems. However, when $\varepsilon \ll 1$, the second order is reduced by logarithmic factors. To identify these factors, we also record (as in [1]) the following quantities

$$C_p^N := N^2 (\ln N)^{-p} D^N, \quad p = 0, 1, 2, 3.. \quad (23)$$

We seek to identify the appropriate value of $p = p^*$ such that $C_{p^*}^N \rightarrow C$ as $N \rightarrow \infty$. In all of the three test problems below, we set $u = 0, (x, y) \in \partial\Omega$.

Example 1 Consider the problem

$$-\varepsilon \Delta u + (2 + x + x^2 + y^2)u_x = 2(2 - x^3)y(1 - y), \quad (x, y) \in \Omega. \quad (24)$$

In this first test example the problem data a, f are smooth and the basic compatibility conditions of $f(\ell, \ell) = 0, \ell = 0, 1$ are satisfied. However, at the inflow corners $f_y(0, \ell) \neq 0, \ell = 0, 1$ and $f_{yy}(x, y) \neq 0, \forall (x, y) \in \Omega$. A sample plot of the computed solution using the numerical scheme (14) is displayed in Figure 1 and the numerical solution is seen to be free of any oscillations. The orders of global convergence for the fitted scheme (14) in Table 1 and Table 2 suggest that the order of convergence is related to an error bound of $CN^{-2}(\ln N)^2$ for this first test problem. The orders of global convergence

Table 1: Orders \bar{p}_ε^N and \bar{p}^N of global convergence for the fitted scheme (14) on the Shishkin mesh Ω^N applied to test problem (24)

εN	$N = 8$	16	32	64	128	256	512
2^0	1.8639	1.9362	1.9661	1.9831	1.9916	1.9958	1.9979
2^{-2}	1.3446	1.6474	1.8130	1.9046	1.9518	1.9758	1.9878
2^{-4}	0.6384	0.9406	1.1919	1.3746	1.5046	1.5948	1.6579
2^{-6}	0.6409	0.9423	1.1915	1.3764	1.5058	1.5956	1.6583
2^{-8}	0.6421	0.9436	1.1914	1.3762	1.5057	1.5956	1.6584
2^{-10}	0.7040	0.9565	1.1937	1.3762	1.5057	1.5955	1.6583
2^{-12}	0.7310	0.9679	1.1981	1.3788	1.5065	1.5957	1.6584
2^{-14}	0.7444	0.9740	1.2005	1.3800	1.5072	1.5961	1.6586
2^{-16}	0.7510	0.9771	1.2018	1.3806	1.5075	1.5963	1.6586
2^{-12}	0.7543	0.9786	1.2025	1.3810	1.5077	1.5964	1.6587
2^{-20}	0.7560	0.9794	1.2029	1.3811	1.5078	1.5964	1.6587
\bar{p}^N	0.7560	0.9794	1.2029	1.3811	1.5078	1.5964	1.6587

Table 2: The quantities (23) for the fitted scheme (14) on the Shishkin mesh Ω^N applied to test problem (24)

$p N$	8	16	32	64	128	256	512
1	0.8916	1.7135	2.8501	4.1597	5.4940	6.7718	7.9673
2	0.4288	0.6180	0.8224	1.0002	1.1323	1.2212	1.2772
3	0.2062	0.2229	0.2373	0.2405	0.2334	0.2202	0.2047

Table 3: Orders \bar{p}_ε^N and \bar{p}^N of global convergence for upwinding on the Shishkin mesh Ω^N applied to test problem (24)

εN	$N = 8$	16	32	64	128	256	512
2^0	1.2089	1.1339	1.0765	1.0401	1.0207	1.0105	1.0053
2^{-2}	0.9809	0.9174	0.9578	0.9770	0.9882	0.9943	0.9972
2^{-4}	0.5089	0.7031	0.7401	0.6967	0.7803	0.8080	0.8331
2^{-6}	0.5188	0.7074	0.7234	0.6937	0.7821	0.8105	0.8353
2^{-8}	0.5204	0.7076	0.7183	0.6922	0.7818	0.8098	0.8355
2^{-10}	0.5660	0.7175	0.7185	0.6918	0.7816	0.8096	0.8355
2^{-12}	0.5835	0.7266	0.7195	0.6949	0.7829	0.8096	0.8356
2^{-14}	0.5920	0.7314	0.7191	0.6965	0.7840	0.8104	0.8358
2^{-16}	0.5961	0.7338	0.7189	0.6974	0.7845	0.8106	0.8360
2^{-18}	0.5982	0.7350	0.7188	0.6979	0.7848	0.8108	0.8361
2^{-20}	0.5992	0.7356	0.7187	0.6982	0.7850	0.8108	0.8361
\bar{p}^N	0.5992	0.7356	0.7187	0.6982	0.7850	0.8108	0.8361

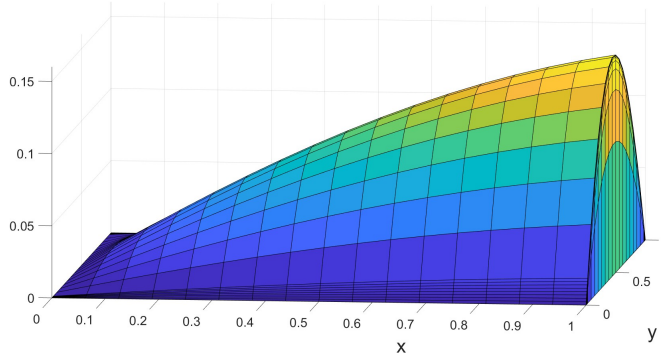


Figure 1: Computed solution (view along $y = 0$) with the numerical scheme (14) applied to problem (24) for $\varepsilon = 2^{-16}$ and $N = 32$

for upwinding on the same mesh in Table 3 indicate $CN^{-1} \ln N$ for the same test problem.

Example 2 Consider the second test problem

$$-\varepsilon \Delta u + (2 + x + x^2 + y^2)u_x = 8(1 - x)y, \quad (x, y) \in \Omega. \quad (25)$$

In this second test example the problem data a, f are smooth, but at the inflow corner $f(0, 1) \neq 0$. A sample plot of the computed solution using the numerical scheme (14) is displayed in Figure 2. The orders of global convergence for the fitted scheme (14) in Tables 4 and 5 suggest that the order of convergence is related to an error bound of $CN^{-2}(\ln N)^3$ for this second test problem.

Example 3 Consider the problem

$$-\varepsilon \Delta u + (1 + x + x^2 + y^2)u_x = 2((2x - 1)(2y - 1))^{\frac{2}{3}} + 4xy^2, \quad (x, y) \in \Omega. \quad (26)$$

In the final test example, we have a non-smooth $f \in C^0(\bar{\Omega}) \setminus C^1(\Omega)$. Even with this low regularity, the method retains higher order uniform convergence (aligned to an error bound of $CN^{-2}(\ln N)^3$), as can be seen in Tables 6 and 7. A sample plot of the computed solution using the numerical scheme (14) is displayed in Figure 3.

From these numerical results, the theoretical constraints being placed on the data in Assumption 4, to establish the global error bounds in Theorem 1, appear to be excessive. Nevertheless, as the constraints on the data are significantly relaxed, we observe a mild degradation in the order of convergence from $N^{-2}(\ln N)^2$ to $N^{-2}(\ln N)^3$.

Table 4: Orders \bar{p}_ε^N and \bar{p}^N of global convergence for the fitted scheme (14) applied to the test problem (25)

εN	$N = 8$	16	32	64	128	256	512
2^0	1.7266	1.8438	1.9032	1.9439	1.9658	1.9791	1.9869
2^{-2}	1.3484	1.6391	1.8097	1.9027	1.9507	1.9752	1.9876
2^{-4}	0.7330	0.9481	1.1875	1.3683	1.4989	1.5909	1.6554
2^{-6}	0.9455	1.1773	1.2136	1.3772	1.5048	1.5933	1.6564
2^{-8}	0.4785	0.9300	1.3797	1.6556	1.8026	1.8926	1.6596
2^{-10}	0.3029	0.2313	0.6440	1.3909	1.6703	1.8107	1.8841
2^{-12}	0.3152	0.2847	0.6309	0.9883	1.2642	1.4441	1.5564
2^{-14}	0.3212	0.2845	0.6310	0.9885	1.2644	1.4442	1.5565
2^{-16}	0.3241	0.2845	0.6310	0.9886	1.2645	1.4443	1.5565
2^{-18}	0.3256	0.2845	0.6310	0.9887	1.2646	1.4444	1.5566
2^{-20}	0.3263	0.2844	0.6310	0.9887	1.2646	1.4444	1.5566
\bar{p}^N	0.2309	0.5317	0.6440	1.0260	1.2317	1.4773	1.5566

Table 5: The quantities (23) for the fitted scheme (14) on the Shishkin mesh Ω^N applied to test problem (25)

$p N$	8	16	32	64	128	256	512
2	3.2961	5.9148	12.4323	22.2994	33.0235	42.0940	48.8850
3	1.5851	2.1333	3.5872	5.3619	6.8061	7.5911	7.8362
4	0.7623	0.7694	1.0350	1.2893	1.4027	1.3690	1.2561

Table 6: Orders \bar{p}_ε^N and \bar{p}^N of global convergence for the fitted scheme (14) applied to the test problem (26)

εN	$N = 8$	16	32	64	128	256	512
2^0	1.7122	1.8712	1.9278	1.9585	1.9778	1.9871	1.9916
2^{-2}	1.4630	1.7098	1.8524	1.9243	1.9623	1.9813	1.9907
2^{-4}	0.5214	0.6999	1.0675	1.6855	1.8375	1.9173	1.9584
2^{-6}	0.8931	0.7915	1.0518	1.2607	1.4343	1.5497	1.6333
2^{-8}	0.5186	1.1380	1.2370	1.2824	1.4359	1.5554	1.6336
2^{-10}	0.2372	0.5428	0.6698	1.4460	1.7392	1.8807	1.9453
2^{-12}	0.2439	0.6109	0.6547	1.0282	1.3127	1.4989	1.6093
2^{-14}	0.2471	0.6181	0.6546	1.0284	1.3129	1.4989	1.6096
2^{-16}	0.2487	0.6217	0.6547	1.0286	1.3131	1.4990	1.6096
2^{-18}	0.2495	0.6235	0.6547	1.0286	1.3131	1.4990	1.6096
2^{-20}	0.2499	0.6245	0.6547	1.0287	1.3131	1.4990	1.6096
\bar{p}^N	0.3185	0.6594	0.6698	1.0615	1.2831	1.5290	1.6096

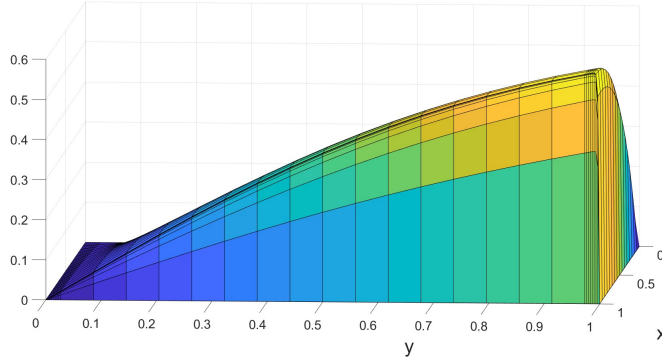


Figure 2: Computed solution (view along $x = 1$) with the numerical scheme (14) applied to problem (25) for $\varepsilon = 2^{-16}$ and $N = 32$

Table 7: The quantities (23) for the fitted scheme (14) on the Shishkin mesh Ω^N applied to test problem (26)

$p N$	8	16	32	64	128	256	512
2	3.8316	7.2498	12.0388	21.2413	30.5973	37.7109	42.1662
3	1.8416	2.6148	3.4737	5.1075	6.3061	6.8007	6.7592
4	0.8861	0.9431	1.0023	1.2281	1.2997	1.2264	1.0835

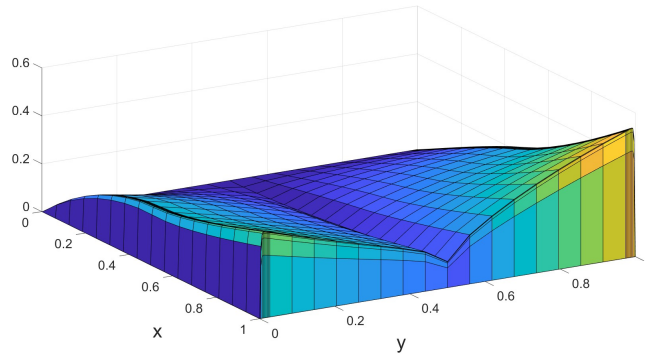


Figure 3: Computed solution (view along $x = 1$) with the numerical scheme (14) applied to problem (26) for $\varepsilon = 2^{-16}$ and $N = 32$

References

- [1] V. B. Andreev, Pointwise approximation of corner singularities for singularly perturbed elliptic problems with characteristic layers, *Int. J.*

- Numer. Anal. Model.*, 7(3), (2010), 416–427.
- [2] V. B. Andreev, Hölder estimates for the regular component of the solution to a singularly perturbed convection-diffusion equation, *Comput. Math. Math. Phys.*, 57(12), (2017), 1935–1972.
- [3] V. B. Andreev and I. G. Belukhina, Estimates in Hölder classes for the solution of an inhomogeneous Dirichlet problem for a singularly perturbed homogeneous convection-diffusion equation, *Comput. Math. Math. Phys.*, 59(2), (2019), 253–265.
- [4] V. B. Andreev and I. G. Belukhina, Decomposition of the solution to a two-dimensional singularly perturbed convection-diffusion equation with variable coefficients in a square and estimates in Hölder norms, *Comput. Math. Math. Phys.*, 61(2), (2021), 194–204.
- [5] P. A. Farrell, A. F. Hegarty, J. J. H. Miller, E. O’Riordan and G. I. Shishkin, *Robust computational techniques for boundary layers*, CRC Press, 2000.
- [6] S. Franz and N. Kopteva, Green’s function estimates for a singularly perturbed convection-diffusion problem, *J. Differential Equations*, 252(2), (2012), 1521–1545.
- [7] S. Franz and H. G. Roos, Error estimation in a balanced norm for a convection-diffusion problem with two different boundary layers, *Calcolo*, 51(3), (2014), 423–440.
- [8] G. M. Gie, C. Y. Jung and R. Temam, Analysis of mixed elliptic and parabolic boundary layers with corners, *Int. J. Differ. Equ.*, (2013), Art. ID 532987, 13.
- [9] H. Han and R. B. Kellogg, Differentiability properties of solutions of the equation $-\epsilon^2 \Delta u + ru = f(x, y)$ in a square, *SIAM J. Math. Anal.*, 21(2), (1990), 394–408.
- [10] A. F. Hegarty and E. O’Riordan, Fitted finite element methods for singularly perturbed elliptic problems of convection-diffusion type, arXiv n: 2310.01237, (2023).
- [11] A. M. Il’in, *Matching of asymptotic expansions of solutions of boundary value problems*, Translations of Mathematical Monographs, 102, American Mathematical Society, Providence, RI, 1992.

- [12] R. B. Kellogg and M. Stynes, Corner singularities and boundary layers in a simple convection-diffusion problem, *J. Differential Equations*, 213(1), (2005), 81–120.
- [13] O. A. Ladyzhenskaya and N. N. Ural'tseva, *Linear and Quasilinear Elliptic Equations*, Academic Press, New York and London, 1968.
- [14] J. J. H. Miller, E. O'Riordan and G. I. Shishkin and L. P. Shishkina, Fitted mesh methods for problems with parabolic boundary layers, *Mathematical Proceedings of Royal Irish Academy*, 98A (2), (1998), 173-190.
- [15] J. J. H. Miller, E. O'Riordan and G. I. Shishkin, *Fitted Numerical Methods for Singular Perturbation Problems*, World-Scientific, Singapore (Revised edition), 2012.
- [16] E. O'Riordan and G. I. Shishkin, Parameter uniform numerical methods for singularly perturbed elliptic problems with parabolic boundary layers, *Applied Numerical Mathematics*, 58, 2008, 1761-1772.
- [17] G. I. Shishkin, A difference scheme for a singularly perturbed equation of parabolic type with a discontinuous boundary condition, *U.S.S.R. Comput. Math. Math. Phys.*, 28(6) , (1988), 32-41.
- [18] G. I. Shishkin, Approximation of solutions of singularly perturbed boundary value problems with a parabolic boundary layer, *U.S.S.R. Comput. Math. Math. Phys.*, 29(4) , (1989), 1-10.
- [19] G. I. Shishkin, On finite difference fitted schemes for singularly perturbed boundary value problems with a parabolic boundary layer, *J. Math. Anal. Appl.*, 208(1), (1997).
- [20] M. Stynes and E. O'Riordan, A uniformly convergent Galerkin method on a Shishkin mesh for a convection-diffusion problem, *J. Math. Anal. Appl.*, 214, 36-54, 1997.

6 Appendix: Truncation error analysis

For the fitted scheme (14) the truncation error is

$$L^N(U - u)(x_i, y_j) = \left((L^N U - f)(x_i, y_j) \right) + \left((L - L^N)u(x_i, y_j) \right)$$

and

$$(L^N U - f)(x_i, y_j) = \frac{1}{2\bar{h}_i} \int_{s=x_{i-1}}^{x_{i+1}} (\bar{f}(s, y_j) - f(x_i, y_j)) ds + \quad (27)$$

$$\frac{1}{\bar{h}_i} \left(\left(\frac{Q_{i,j}^-}{h_i} - \frac{1}{2} \right) \int_{s=x_{i-1}}^{x_i} \bar{f}(s, y_j) ds + \left(\frac{Q_{i,j}^+}{h_{i+1}} - \frac{1}{2} \right) \int_{s=x_i}^{x_{i+1}} \bar{f}(s, y_j) ds \right).$$

We next examine the term $(L - L^N)u(x_i, y_j)$. In the special case of $h_i = h_{i+1}$ we note that

$$D_x^- u_i = D_x^0 u_i - \frac{h_i}{2} \delta_x^2 u_i, \quad \text{where} \quad D_x^0 u_i := \frac{u_{i+1} - u_{i-1}}{2h_i}.$$

This motivates the following rearrangement of the terms in the fitted operator component of L^N in (15) :

$$\begin{aligned} & (-\varepsilon h_{i+1} D_x^+ (\sigma(-\rho_{i,j}) D_x^-) + \bar{a} h_i D_x^-) U(x_i, y_j) \\ &= (-\varepsilon h_{i+1} D_x^+ (\sigma(-\rho_{i,j}) + \frac{\rho_{i,j}}{2} D_x^-) U(x_i, y_j) + \bar{h}_i a(x_i, y_j) D_x^0 U(x_i, y_j) \\ &+ ((\bar{a}_{i+1}(y_j) - a(x_i, y_j)) \frac{h_{i+1}}{2} D_x^+ + (\bar{a}_i(y_j) - a(x_i, y_j)) \frac{h_i}{2} D_x^-) U(x_i, y_j) \\ &= \bar{h}_i (-\varepsilon \delta_x^2 + a D_x^0) U(x_i, y_j) + (-\varepsilon h_{i+1} D_x^+ (\frac{\rho_{i,j}}{2} \coth(\frac{\rho_{i,j}}{2}) - 1) D_x^-) U(x_i, y_j) \\ &+ ((a(x_{i+1}, y_j) - a(x_i, y_j)) \frac{h_{i+1}}{4} D_x^+ - (a(x_i, y_j) - a(x_{i-1}, y_j)) \frac{h_i}{4} D_x^-) U(x_i, y_j). \end{aligned}$$

Using this rearrangement, we have that

$$\begin{aligned} (L - L^N)u(x_i, y_j) &= (\varepsilon(\delta_x^2 u - u_{xx}) + \varepsilon(\delta_y^2 u - u_{yy}) + a(u_x - D_x^0 u))(x_i, y_j) \\ &+ (\varepsilon \frac{h_{i+1}}{\bar{h}_i} D_x^+ (\frac{\rho_{i,j}}{2} \coth(\frac{\rho_{i,j}}{2}) - 1) D_x^-) u(x_i, y_j) + (1 - \frac{Q_{i,j}^C}{\bar{h}_i})(-\varepsilon \delta_y^2) u(x_i, y_j) \\ &- ((a(x_{i+1}, y_j) - a(x_i, y_j)) \frac{h_{i+1}}{4\bar{h}_i} D_x^+ - (a(x_i, y_j) - a(x_{i-1}, y_j)) \frac{h_i}{4\bar{h}_i} D_x^-) u(x_i, y_j) \\ &= (\varepsilon(\delta_x^2 u - u_{xx}) + \varepsilon(\delta_y^2 u - u_{yy}) + a(u_x - D_x^0 u))(x_i, y_j) + (1 - \frac{Q_{i,j}^C}{\bar{h}_i})(-\varepsilon \delta_y^2) u(x_i, y_j) \\ &+ \frac{\bar{a}_{i+1,j}}{2} (\coth(\frac{\rho_{i+1,j}}{2}) - \frac{2}{\rho_{i+1,j}}) \frac{h_{i+1}}{\bar{h}_i} D_x^+ - \frac{\bar{a}_{i,j}}{2} (\coth(\frac{\rho_{i,j}}{2}) - \frac{2}{\rho_{i,j}}) \frac{h_i}{\bar{h}_i} D_x^- \\ &- ((a(x_{i+1}, y_j) - a(x_i, y_j)) \frac{h_{i+1}}{4\bar{h}_i} D_x^+ - (a(x_i, y_j) - a(x_{i-1}, y_j)) \frac{h_i}{4\bar{h}_i} D_x^-) u(x_i, y_j). \end{aligned}$$

$$\begin{aligned}
&= (\varepsilon(\delta_x^2 u - u_{xx}) + \varepsilon(\delta_y^2 u - u_{yy}) + a(u_x - D_x^0 u))(x_i, y_j) \\
&\quad - ((a(x_{i+1}, y_j) - a(x_i, y_j)) \frac{h_{i+1}}{4h_i} D_x^+ - (a(x_i, y_j) - a(x_{i-1}, y_j)) \frac{h_i}{4h_i} D_x^-) u(x_i, y_j) \\
&\quad + \frac{1}{h_i} \left(\left(\frac{1}{2} - \frac{Q_{i,j}^-}{h_i} \right) \int_{x=x_{i-1}}^{x_i} (\bar{a}(y_j) D_x^- - \varepsilon \delta_y^2) u(x_i, y_j) dx \right) \\
&\quad + \frac{1}{h_i} \left(\left(\frac{1}{2} - \frac{Q_{i,j}^+}{h_{i+1}} \right) \int_{x=x_i}^{x_{i+1}} (\bar{a}(y_j) D_x^+ - \varepsilon \delta_y^2) u(x_i, y_j) dx \right), \tag{28}
\end{aligned}$$

as

$$\frac{Q_{i,j}^-}{h_i} - \frac{1}{2} = \frac{1}{2} \coth\left(\frac{\rho_{i,j}}{2}\right) - \frac{1}{\rho_{i,j}}; \quad \frac{1}{2} - \frac{Q_{i,j}^+}{h_{i+1}} = \frac{1}{2} \coth\left(\frac{\rho_{i+1,j}}{2}\right) - \frac{1}{\rho_{i+1,j}}.$$

We now combine the two contributions (27) and (28) to the truncation error, to get

$$L^N(U - u)(x_i, y_j) = (T_1 - T_2 + T_3 + T_4)(x_i, y_j), \quad \text{where}$$

$$T_1(x_i, y_j) := (\varepsilon(\delta_x^2 u - u_{xx}) + \varepsilon(\delta_y^2 u - u_{yy}) + a(u_x - D_x^0 u))(x_i, y_j); \tag{29a}$$

$$\begin{aligned}
T_2(x_i, y_j) &:= (a(x_{i+1}, y_j) - a(x_i, y_j)) \frac{h_{i+1}}{4h_i} D_x^+ u(x_i, y_j) \\
&\quad - (a(x_i, y_j) - a(x_{i-1}, y_j)) \frac{h_i}{4h_i} D_x^- u(x_i, y_j); \tag{29b}
\end{aligned}$$

$$T_3(x_i, y_j) := \frac{1}{2h_i} \int_{s=x_{i-1}}^{x_{i+1}} (\bar{f}(s, y_j) - f(x_i, y_j)) ds; \tag{29c}$$

$$\begin{aligned}
T_4(x_i, y_j) &:= \frac{1}{h_i} \left(\left(\frac{1}{2} - \frac{Q_{i,j}^-}{h_i} \right) \int_{s=x_{i-1}}^{x_i} \left((\bar{a} D_x^- - \varepsilon \delta_y^2) u - \bar{f} \right) (s, y_j) ds \right. \\
&\quad \left. + \left(\frac{1}{2} - \frac{Q_{i,j}^+}{h_{i+1}} \right) \int_{s=x_i}^{x_{i+1}} \left((\bar{a} D_x^+ - \varepsilon \delta_y^2) u - \bar{f} \right) (s, y_j) ds \right). \tag{29d}
\end{aligned}$$

We next separately bound each of the four terms $T_i, i = 1, 2, 3, 4$, which contribute to the truncation error. Use standard truncation error bounds to bound the terms in T_1 . Note the terms T_2 in (29b) are

$$\begin{aligned}
&= \frac{(h_{i+1}^2 - h_i^2) a_x u_x}{4h_i} + a_x \frac{(h_{i+1}^2 (D_x^+ - u_x) - h_i^2 (D_x^- - u_x)) u(x_i, y_j)}{4h_i} \\
&\quad + ((a(x_{i+1}, y_j) - (a + h_{i+1} a_x)(x_i, y_j)) \frac{h_{i+1}}{4h_i} D_x^+ u(x_i, y_j) \\
&\quad - ((a - h_i a_x)(x_i, y_j) - a(x_{i-1}, y_j)) \frac{h_i}{4h_i} D_x^- u(x_i, y_j)).
\end{aligned}$$

Thus

$$|T_2(x_i, y_j)| \leq C(h_i - h_{i+1})\|u_x\|_i + Ch_i^2(\|u_{xx}\|_i + \|u_x\|_i),$$

where, throughout this appendix, we adopt the notation

$$\|f(y_j)\|_i := \max_{s \in (x_{i-1}, x_{i+1})} |f(s, y_j)| \quad \text{and} \quad \|f(x_i)\|_j := \max_{s \in (y_{j-1}, y_{j+1})} |f(x_i, s)|.$$

We also have

$$|T_3(x_i, y_j)| \leq \left| \frac{C}{\bar{h}_i} \int_{s=x_{i-1}}^{x_{i+1}} (\bar{f}(s, y_j) - f(x_i, y_j)) ds \right| \leq C(h_i - h_{i+1}) + Ch_i^2.$$

It remains to bound the term $T_4(x_i, y_j)$ (29d). From the differential equation we have that

$$-\varepsilon u_{yy} + au_x - f = \varepsilon u_{xx} \quad \text{and} \quad (au_x - f)_x = \varepsilon(u_{xx} + u_{yy})_x.$$

Hence,

$$\begin{aligned} & (\bar{a}_{i+1}(y_j)D_x^+ - \varepsilon\delta_y^2)u(x_i, y_j) - \bar{f}_{i+1}(y_j) = (-\varepsilon u_{yy} + au_x - f)(x_i, y_j) \\ & + ((\bar{a}_{i+1}(y_j) - a(x_i, y_j))D_x^+)u(x_i, y_j) + f(x_i, y_j) - \bar{f}_{i+1}(y_j) \\ & - \varepsilon(\delta_y^2 u - u_{yy}) - a(u_x - D_x^+ u)(x_i, y_j) \\ = & (\varepsilon u_{xx} + \frac{h_{i+1}}{2}(au_{xx} + a_x u_x - f_x) - \varepsilon(\delta_y^2 u - u_{yy}))(x_i, y_j) \\ & + ((\bar{a}_{i+1}(y_j) - (a + \frac{h_{i+1}}{2}a_x)(x_i, y_j))D_x^+)u(x_i, y_j) + (f + \frac{h_{i+1}}{2}f_x)(x_i, y_j) - \bar{f}_{i+1}(y_j) \\ & - a(u_x + \frac{h_{i+1}}{2}u_{xx} - D_x^+ u)(x_i, y_j) + \frac{h_{i+1}}{2}a_x(D_x^+ u - u_x)(x_i, y_j); \\ = & (\varepsilon u_{xx} + \frac{h_{i+1}}{2}(\varepsilon(u_{xx} + u_{yy})_x) - \varepsilon(\delta_y^2 u - u_{yy}))(x_i, y_j) \\ & + ((\bar{a}_{i+1}(y_j) - (a + \frac{h_{i+1}}{2}a_x)(x_i, y_j))D_x^+)u(x_i, y_j) + (f + \frac{h_{i+1}}{2}f_x)(x_i, y_j) - \bar{f}_{i+1}(y_j) \\ & - a(u_x + \frac{h_{i+1}}{2}u_{xx} - D_x^+ u)(x_i, y_j) + \frac{h_{i+1}}{2}a_x(D_x^+ u - u_x)(x_i, y_j). \end{aligned}$$

In an analogous fashion

$$\begin{aligned}
& (\bar{a}_i(y_j)D_x^- - \varepsilon\delta_y^2)u(x_i, y_j) - \bar{f}_i(y_j) = (-\varepsilon u_{yy} + au_x - f)(x_i, y_j) \\
& + ((\bar{a}_i(y_j) - a(x_i, y_j))D_x^-)u(x_i, y_j) + f(x_i, y_j) - \bar{f}_i(y_j) \\
& - \varepsilon(\delta_y^2 u - u_{yy}) - a(u_x - D_x^- u)(x_i, y_j) \\
= & (\varepsilon u_{xx} - \frac{h_i}{2}(\varepsilon(u_{xx} + u_{yy})_x) - \varepsilon(\delta_y^2 u - u_{yy}))(x_i, y_j) \\
& + ((\bar{a}_i(y_j) - (a - \frac{h_i}{2}a_x)(x_i, y_j))D_x^-)u(x_i, y_j) + (f - \frac{h_i}{2}f_x)(x_i, y_j) - \bar{f}_i(y_j) \\
& - a(u_x - \frac{h_i}{2}u_{xx} - D_x^- u)(x_i, y_j) - \frac{h_i}{2}a_x(D_x^- u - u_x)(x_i, y_j).
\end{aligned}$$

Moreover

$$\frac{1}{\bar{h}_i} \left(\left(\frac{1}{2} - \frac{Q_{i,j}^-}{h_i} \right) \int_{x=x_{i-1}}^{x_i} dx + \left(\frac{1}{2} - \frac{Q_{i,j}^+}{h_{i+1}} \right) \int_{x=x_i}^{x_{i+1}} dx \right) = 1 - \frac{Q_{i,j}^C}{\bar{h}_i}.$$

From these expressions, we have that the terms in (29d) are bounded by

$$\begin{aligned}
|T_4(x_i, y_j)| & \leq Ch_i^2 (\|u_{xxx}(y_j)\|_i + \|u_{xx}(y_j)\|_i + \|u_x(y_j)\|_i + 1) \\
& + C\varepsilon \left| 1 - \frac{Q_{i,j}^C}{\bar{h}_i} \right| (\|u_{xx}(x_i, y_j)\| + \|(\delta_y^2 u - u_{yy})(x_i)\|_j) \\
& + |((au_x - f)_x(x_i, y_j)) \left(\frac{h_{i+1}^2}{2\bar{h}_i} \left(\frac{1}{2} - \frac{Q_{i,j}^+}{h_{i+1}} \right) - \frac{h_i^2}{2\bar{h}_i} \left(\frac{1}{2} - \frac{Q_{i,j}^-}{h_i} \right) \right)|.
\end{aligned}$$

Note that

$$\left| \left(\frac{1 - \sigma(-x)}{x} \right)' \right| \leq C \min\{1, \frac{1}{x}\}.$$

Using this inequality we have that

$$\left| 1 - \frac{Q_{i,j}^C}{\bar{h}_i} \right| = \left| \frac{1 - \sigma(-\rho_{i,j})}{\rho_{i,j}} - \frac{1 - \sigma(-\rho_{i+1,j})}{\rho_{i+1,j}} \right| \leq Ch_i \min\{1, \frac{h_i}{\varepsilon}\}, \quad \text{if } x_i \neq 1 - \tau_\varepsilon; \tag{30a}$$

and at the transition point

$$1 - \frac{Q_{i,j}^C}{\bar{h}_i} = \frac{h_i}{2\bar{h}_i} \left(\frac{1 - \sigma(-\rho_{i,j})}{\rho_{i,j}} - \frac{\sigma(\rho_{i,j}) - 1}{\rho_{i,j}} \right) + \frac{h_{i+1}}{2\bar{h}_i} \left(\frac{\sigma(\rho_{i+1,j}) - 1}{\rho_{i+1,j}} - \frac{1 - \sigma(-\rho_{i+1,j})}{\rho_{i+1,j}} \right).$$

Using $|x \coth x - 1| \leq Cx^2$, we deduce that

$$\left| 1 - \frac{Q_{i,j}^C}{\bar{h}_i} \right| \leq C \min\{1, \frac{h_i}{\varepsilon}\} \quad \text{if } x_i = 1 - \tau_\varepsilon. \tag{30b}$$

In addition,

$$\begin{aligned}
h_i Q_{i,j}^- - h_{i+1} Q_{i,j}^+ &= h_i^2 \left(\frac{Q_{i,j}^-}{h_i} - \frac{1}{2} \right) - h_{i+1}^2 \left(\frac{Q_{i,j}^+}{h_i} - \frac{1}{2} \right) + \frac{h_i^2 - h_{i+1}^2}{2}, \\
\frac{Q_{i,j}^+}{h_{i+1}} - \frac{Q_{i,j}^-}{h_i} &= \frac{1 - \sigma(-\rho_{i+1,j})}{\rho_{i+1,j}} - \frac{1 - \sigma(-\rho_{i,j})}{\rho_{i,j}} + \frac{2}{\rho_{i,j}} \left(1 - \frac{\rho_{i,j}}{2} \coth \frac{\rho_{i,j}}{2} \right), \\
\left| \frac{Q_{i,j}^+}{h_{i+1}} - \frac{Q_{i,j}^-}{h_i} \right| &\leq C \min\{1, \frac{h_i}{\varepsilon}\}.
\end{aligned}$$

Hence,

$$\left| \frac{h_{i+1}^2}{h_i} \left(\frac{1}{2} - \frac{Q_{i,j}^+}{h_{i+1}} \right) - \frac{h_i^2}{h_i} \left(\frac{1}{2} - \frac{Q_{i,j}^-}{h_i} \right) \right| \leq C h_i \min\{1, \frac{h_i}{\varepsilon}\} + C |h_i - h_{i+1}|. \quad (30c)$$

Using the three inequalities in (30) to bound $T_4(x_i, y_j)$, we arrive at the following truncation error bounds: If $h_i = h_{i+1}$, then

$$\begin{aligned}
|L^N(U - u)(x_i, y_j)| &\leq C h_i^2 (\varepsilon \left\| \frac{\partial^4 u}{\partial x^4}(y_j) \right\|_i + \sum_{n=1}^3 \left\| \frac{\partial^n u}{\partial x^n}(y_j) \right\|_i + 1) + \varepsilon \|\delta_y^2 u - u_{yy}(x_i)\|_j \\
&+ C h_i \min\{1, \frac{h_i}{\varepsilon}\} \varepsilon \left(\left| \frac{\partial^3 u}{\partial x^3}(x_i, y_j) \right| + \left| \frac{\partial^3 u}{\partial y^2 \partial x}(x_i, y_j) \right| + \left| \frac{\partial^2 u}{\partial x^2}(x_i, y_j) \right| \right) \quad (31)
\end{aligned}$$

and at all mesh points (including the transition point)

$$\begin{aligned}
|L^N(U - u)(x_i, y_j)| &\leq C h_i (\varepsilon \left\| \frac{\partial^3 u}{\partial x^3}(y_j) \right\|_i + \sum_{n=1}^2 \left\| \frac{\partial^n u}{\partial x^n}(y_j) \right\|_i + 1) + \varepsilon \|\delta_y^2 u - u_{yy}(x_i)\|_j \\
&+ C h_i^2 \left\| \frac{\partial^3 u}{\partial x^3}(y_j) \right\|_i + C \min\{\varepsilon, h_i\} \left| \frac{\partial^2 u}{\partial x^2}(x_i, y_j) \right|. \quad (32)
\end{aligned}$$

Note finally that

$$\|\delta_y^2 u - u_{yy}\| \leq C \bar{k}_j \begin{cases} \min\{\|u_{yyy}\|, \bar{k}_j \|u_{yyyy}\|\}, & \text{if } k_j = k_{j+1} \\ \|u_{yyy}\|, & \text{if } k_j \neq k_{j+1} \end{cases}.$$